Manuscript: egusphere-2023-1808

Title: Alternative climatic steady states for the Permian-Triassic paleogeography

Reviewer #2:

Ragon and others explore climate of the Permian-Triassic with the MITGCM. They find three equilibrium climate states with an initial CO_2 of 320 ppm. From these initial states, they explore the range of stability and the importance of vegetation and carbon cycle feedbacks.

I found this to be an interesting study. The experiment design was well thought out. The text and figures were easy to follow. Here are some comments that I think could improve the manuscript.

We are grateful for this positive evaluation of our study.

A lot of steps went into the model spin up. They are well documented in the text, which I appreciate. Although the text is generally clear, I think a schematic of the spin up procedure would help the reader understand what was done.

We thank the reviewer for this suggestion. We can add the following schematic for the whole procedure in a new appendix (or in Supplementary Material).
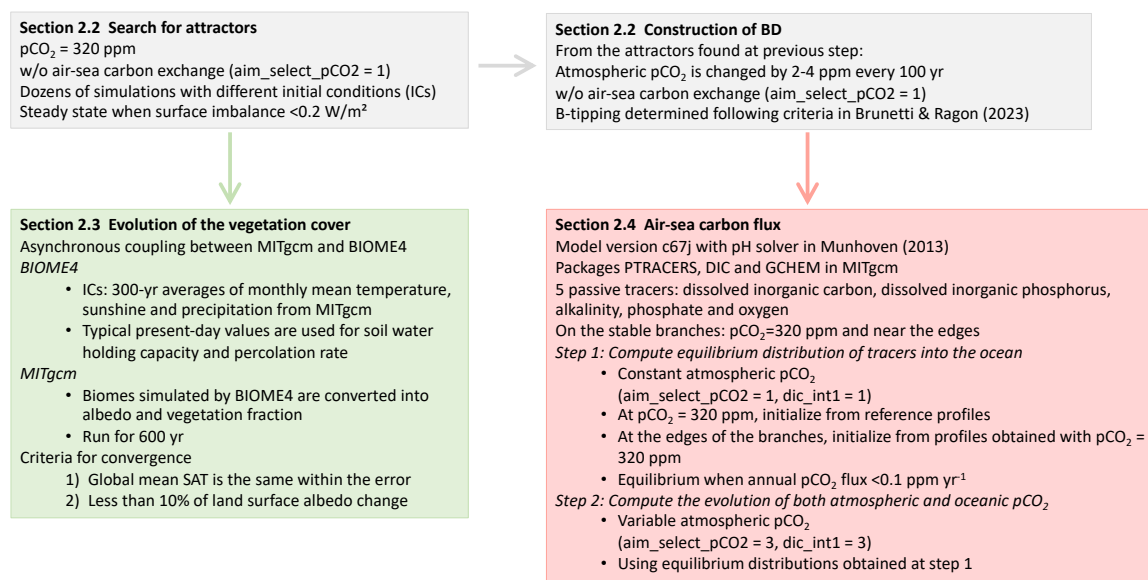

Figure 1: Schematic of the numerical procedure.

There was a lot of work put into creating realistic boundary conditions. This is worthwhile since most previous MITGCM multiple equilibria studies used idealized configurations. One of the benefits of realistic boundary conditions is model-proxy comparison. The authors speculate that the mismatch between HadCM3 simulations and a proxy reconstruction might be the result of multiple equilibria. However, the authors do not make any model-proxy comparisons themselves. I do not think many temperature records of the Permian-Triassic exist, but it is still worth doing.

We suggest to add a new paragraph in the Introduction (at line 40) to better explain the context of our numerical simulations:

We are interested in the climatic oscillations observed at the Smithian-Spathian boundary in the Early Triassic, just after the Permian-Triassic boundary (PTB) mass extinction ($\sim$252 Ma), the most severe of the Phanerozoic (Raup, 1979; MacLeod, 2014; Stanley, 2016). As a consequence of the volcanic activity of the Siberian Large Igneous Province (Campbell et al., 1992; Renne et al., 1995; Reichow et al., 2009), the global carbon cycle entered a perturbed state which persisted for nearly 5.4 Myr in the Early Triassic, until a new equilibrium state was reached in the Anisian (Sun et al., 2012; Romano et al., 2013; Goudemand et al., 2019; Leu et al., 2019; Widmann et al., 2020). The observed fluctuations in the carbon isotope

record (Payne et al., 2004; Galfetti et al., 2007; Retallack et al., 2011) with successive diversification-extinction cycles of the nekton (Orchard, 2007; Brühwiler et al., 2010; Leu et al., 2019) and ecological crises of terrestrial plants (Hermann et al., 2011; Schneebeli-Hermann, 2020), are all indicative of the climatic changes which occurred in the Early Triassic, with variations in the global temperature of the order of 7-8 °C from the thermal maximum in the late Smithian to cold climates in early Spathian times (Widmann et al., 2020).

However, despite the great effort of the scientific community to reconstruct such climatic oscillations in the aftermath of the PTB, large uncertainties remain in timing and causal relationships, implying that numerical modelling needs to consider a wide range of initial and boundary conditions for the simulation of such geological interval. In this context, ... [continuing at line 44]

A detailed comparison between biomes and plant fossil data goes well beyond the scope of the present work. We are preparing such comparison for a forthcoming publication. The aim of the present work is to focus on the climatic states that we obtain with the same paleogeography and different initial conditions, in order to open the possibility of using alternative steady states and tipping mechanisms in future proxy comparisons for the Early Triassic.

On the point of realism, the range of CO_2 for these equilibrium states is quite small from a geologic perspective. What are the implications of this?

The atmospheric module is based on SPEEDY, the Simplified Parametrizations primitivE-Equation DYnamics described in Molteni (2003) (see also the Appendix to that article on the web page of SPEEDY). In the parameterization scheme for the longwave radiation, the infrared spectrum is partitioned into four regions: 1) the 'infrared window' between 8.5 and 11 μm; 2) the band of strong absorption by CO_2 around 15 μm; 3) the aggregation of regions with weak/moderate absorption by water vapour; 4) the aggregation of regions with strong absorption by water vapour. Thus, the absorption of CO_2 is limited by the fact that only the largest absorption band is included in the infrared spectrum. This implies that the atmospheric CO_2 content is probably underestimated in our simulations, and that the range of CO_2 for the steady states can change when considering the full absorption bands. We propose to include this more detailed description of the infrared spectrum in SPEEDY in Section 2.1.

Another aspect to consider is that the various estimates for pCO_2 content around the Permian-Triassic Boundary and Early Triassic (e. g. Royer et al. (2004); Berner (2006); Foster et al. (2017); Lenton et al. (2018); Joachimski et al. (2022)) have relatively low values for the Phanerozoic with large error bars. As mentioned in the manuscript at line 100, Fig. 1 (and corresponding data in Supplementary Material) in Foster et al. (2017) shows huge uncertainties for the Early Triassic, with CO_2 values ranging between 0 and 1800 ppm.

Also, a few sentences of discussion about the biomes of the Permian-Triassic versus the biomes in BIOME4 would be worthwhile.

BIOME4 is based on the concept of Plant Funcional Type (PFT), rather than taxonomic grouping (Kaplan, 2001). Despite the definition of PFTs is based on present-day plants, this is the only available framework that can be applied to plants at different deep-time geological periods, assuming that their functionality was similar to the present-day one. Within this framework, plants with certain fundamental characteristis (*i. e.*, growth form, phenology, rooting depth) are grouped together and included in BIOME4, allowing for studying their distribution at the global scale. BIOME4 has been applied to study the Jurassic climate (Sellwood & Valdes, 2008), the Middle Pliocene (3.6-2.6 Ma; Salzmann et al. (2008)), the Last Glacial Maximum (Harrison & Prentice, 2003). We suggest to include the concept of PFTs and relevant literature in Section 2.3.

As said above, we are presently comparing our simulation results with plant fossil data. For the forthcoming study, we will adapt the output of BIOME4 to biomes defined as in Ziegler (1990) and Nowak et al. (2020). Such definition is more general and applicable to the Permian-Triassic period. However, in the present study we prefer to consider the same definition of mega-biomes as in many other studies of the past, as mentioned in the previous paragraph.

Line 81-82: Can you provide a bit more information about how the model conserves energy?

The energy conservation of the MITgcm has been investigated by Campin et al. (2008) in coupled simulations. The accuracy to which heat is conserved (but also salt and fresh water) is limited by machine precision, with a time-stepping implementation which turns out to be stable and conservative. We have further investigated the energy conservation issue in our MITgcm setup in Brunetti & Vérard (2018); Brunetti et al. (2019); Ragon et al. (2022). As discussed in Lucarini & Ragone (2011), even if a model can perfectly conserve energy between its components at the ocean surface, as the MITgcm does, it can still have energy sources/sinks that affect the TOA budget, that are not accounted for and are sometimes

called 'ghost energy' (Pascale et al., 2012). As discussed in Lucarini & Ragone (2011) and Liepert & Previdi (2012), the spurious bias is due to physical processes that have been neglected, inconsistently treated, or approximated in climate models, as well as to unphysical effects of numerical dissipation (Pascale et al., 2012; Mauritsen et al., 2012; Lauritzen & Williamson, 2019; Trenberth, 2020). The TOA energy balance ranges between -0.2 and 4.8 W/m^2 in the preindustrial scenario with CMIP3 (as shown in Fig. 2A in Lucarini & Ragone (2011)), and between -3.16 and 2.37 in CMIP5 (see Table 2 in Lembo et al. (2019)). In our setting, the range is between -0.4 and -0.1 W/m^2 (see Table 3), and the ocean surface energy imbalance is less than 0.1 W/m^2 in absolute value, since we run the simulations towards equilibrium. The main contribution to TOA energy imbalance comes from the fact that sea ice dynamics is neglected in our setup (Brunetti & Vérard, 2018). We have discussed these conservation properties in our previous papers (Brunetti & Vérard, 2018; Brunetti et al., 2019; Ragon et al., 2022). We can refer to these papers in the revised manuscript and add some more information on energy conservation in our Permian-Triassic setup in Section 3.

Line 84: I do not think Foster et al. (2017) is the original source. Maybe Gough (1981)?

The original reference is indeed Gough (1981), and Foster et al. (2017) refer to this paper.

Line 106: Is it possible the tipping points could occur with less forcing if the simulations were run for more than 100 years?

The trade-off between the increase in forcing ΔS and the interval of time ΔT is discussed in Brunetti & Ragon (2023) (Method II). The change of the forcing ΔS should be sufficiently low to avoid rate-induced tipping (R-tipping). On the other hand, this method becomes interesting from the point of view of reducing the computational time if ΔT is not too large. We have tested different values in a coupled aquaplanet configuration, where the bifurcation diagram is obtained with large relaxation times (standard method in Brunetti & Ragon (2023)). We saw that taking $\Delta T \sim 100$ yr was sufficient to reconstruct well the position of tipping points. This is why we have used the same value here. If ΔT is increased, with ΔS sufficiently small to avoid R-tipping, the estimated position of the tipping point can slightly change, but the overall picture of the bifurcation diagram remains the same. The larger ΔT, the more precise the position of tipping points, the higher the computational cost.

Line 119: Is there any transpiration component in the MITgcm?

Transpiration is not taken into account in the MITgcm atmospheric module. We can add this information in the model description (Section 3.1).

Line 123: "run BIOME4 again"

We thank the reviewer for pointing out this typo.

Line 143: 0.1 ppm per year seems like a large drift on geologic time scales. Does it look like the carbon is heading towards an equilibrium or continually drifting?

A value smaller than 0.1 ppm/yr is required only at the end of the first step. At the final step, the equilibrium values are reported in Table 5 and are consistent with a null flux (within uncertainties). We suggest to reformulate this sentence at step 1, the paragraph at step 2 and the footnote by avoiding the word 'equilibrium', which is misleading in this context.

Line 203: "to simulate larger pCO2 values"

This sentence will be corrected indeed as suggested.

Line 204: To clarify, the model boundary conditions are largely responsible for the high temperature sensitivity?

The reviewer is right: the boundary conditions (the Permian-Triassic paleogeography) have an impact on the temperature of the steady states, for the same CO_2 content. Using boundary conditions for an aquaplanet gives steady states with different global mean temperatures (Brunetti et al., 2019; Brunetti & Ragon, 2023). However, the numerical instability that we observe at mean global surface air temperatures larger than 38 °C does not depend on such boundary conditions, but on the atmospheric module of MITgcm (SPEEDY, based on simplified parametrizations described in Section 2.1; see also Molteni (2003)).

Line 212: Based on Figure B1, it does not seem like the cold state can be reached from the warm state, so the loop is not closed. What are the implications of this with respect to real climate evolution?

The cold state stability range extends beyond the warm state branch on both sides, as it can be seen in Fig. 11 where only stable regions have been shown. Thus, the cold state can be reached from the warm state through bifurcation-induced tipping (B-tipping). However, the warm state cannot be reached

from the cold state by B-tipping, as we say at lines 207-208. Implications are that the warm state can in principle be attained through other tipping mechanisms, as for example noise-induced tipping due to perturbations of the biological pump. As we state in the manuscript (lines 209-210), if we assume that the size of the warm state basin of attraction is proportional to the branch length, catching the warm attractor would require very specific initial conditions and is therefore quite unlikely to occur.

Line 216: I do not follow this argument. HadCM3, like other higher complexity models, does not produce multiple equilibria. CO2 and proxy reconstruction uncertainties seem more probably explanations for the mismatch. Are you arguing that HadCM3 is somehow stuck in a cold equilibrium solution? Also, is it OK to cite an EGU presentation?

We disagree with the reviewer, since nowadays several high compexity models show mutiple equilibria. For example, the eddy-permitting GCM HadGEM3-GC2 shows hysteresis of the Atlantic Meridional Over-turning Circulation over centennial time scales (Jackson & Wood, 2018). Similarly, Peltier & Vettoretti (2014) show abrupt transitions in CESM1 over millennial time scales. A result that has been repeated by a number of other IPCC-class models (see review by Malmierca-Vallet et al. (2023)), including HadCM3B. Hence higher complexity models are indeed able to produce multiple equilibria.

On the discrepancy between simulation results and proxy data, we discussed at EGU2023 with Prof. Paul Valdes, who is now interested in performing additional numerical simulations with HadCM3 to explore the hypothesis of the presence of multiple steady states under the same Permian-Triassic boundary conditions. Unfortunately, he has not had time until now to publish a paper about that, thus we can only cite his presentation at EGU, which anyway has a doi number. We can also add: 'Paul Valdes, *personal communication*'.

Table 3: I am confused by the differences in energy balance between the ocean surface and TOA. Where is the energy going?

See the point above on the energy conservation (lines 81-82). The surface energy balance becomes nearly zero if simulations are long enough, as in our case where the simulations are run towards equilibrium. The TOA energy balance can be affected by the so-called 'ghost energy', mainly due to numerical dissipation or missed processes in the simulation setup (Lucarini & Ragone, 2011; Brunetti & Vérard, 2018). In our simulations, the TOA budget ranges between -0.4 and -0.1 W/m2 (see Table 3), which are small values in comparison to those obtained by some CMIP models (see references above).

Some of the figures would be easier to interpret with difference plots. I think figures 7, 8, and 9 in particular.

We thank the reviewer for this suggestion. Difference plots indeed improve the comparison of precipitation and evaporation, especially in warm and cold states where these quantities are quite similar, as shown below (Fig. 2 in this response).
Regarding the salinity field, we think that difference plots are not useful (see Fig. 3 below), since we are interested to show that the salinity distribution is symmetrical in the hot state with respect to the Equator because of the absence of ice. Thus, we prefer not to use difference plots for the salinity. Instead, contour lines can be added to improve readability (Fig. 4 below).

Figure D1: I do not understand the temperature response with the carbon cycle. Why does the sensitivity change, especially in the warm state? Also, I am surprised that turning on the carbon cycle did not lead to large changes in atmospheric CO2. Any explanation?

The stable branch of the warm state is very short, and thus a small perturbation in the forcing can easily induce a loss of the steady state. This indeed is what happens by including air-sea carbon exchanges. The warm state looses stability on the (short) branch. In contrast, the climate sensitivity of the other two steady states does not change much when air-sea carbon exchanges are allowed.
The fact that allowing carbon exchanges only slightly affects the atmospheric CO_2 content (and the equilibrium temperature) is due to the procedure used, which is described in section 2.3. We first estimate the distributions of oceanic tracers (DIC, dissolved inorganic phosphorous, alkalinity, phosphate and oxygen), which correspond to given values of atmospheric CO_2 content on the stable branch of the attractors (step 1). Then, these distributions are used when the air-sea carbon exchange is allowed (step 2). By construction, air-sea carbon exchanges vary the atmospheric CO_2 content of the order of 10 ppm (see Table 5). The advantage of including the option of CO_2 exchanges is to obtain the total (ocean + atmosphere) carbon content for each state, as reported in Table 5.
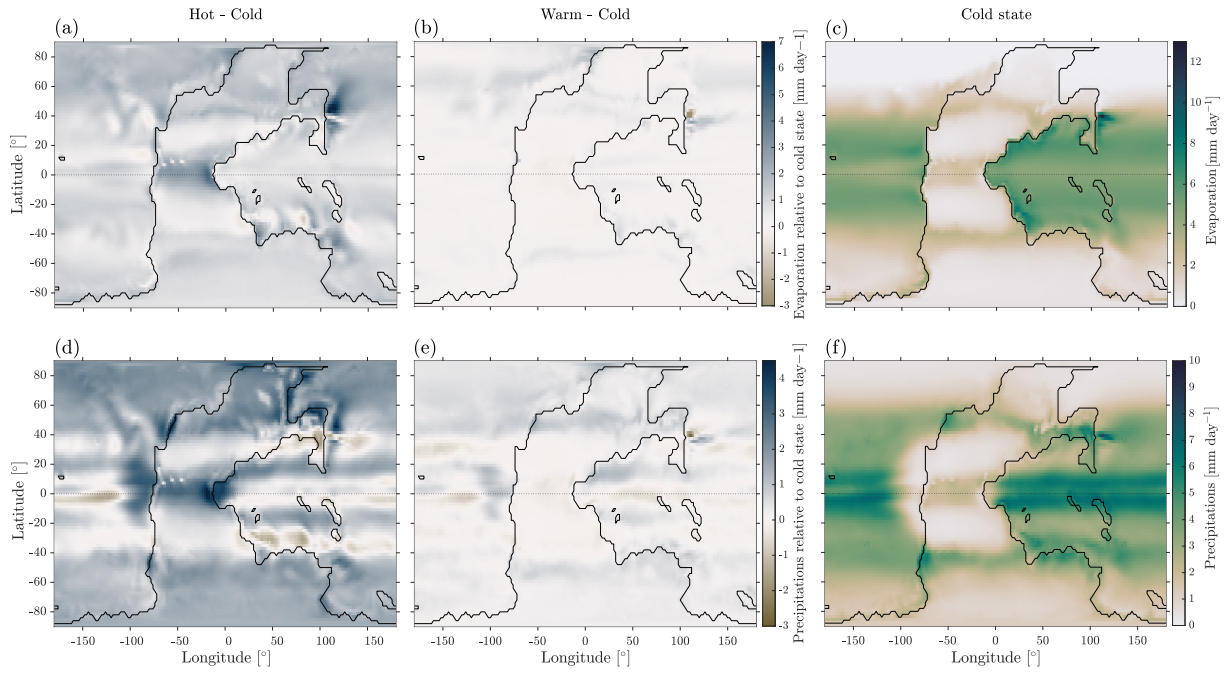
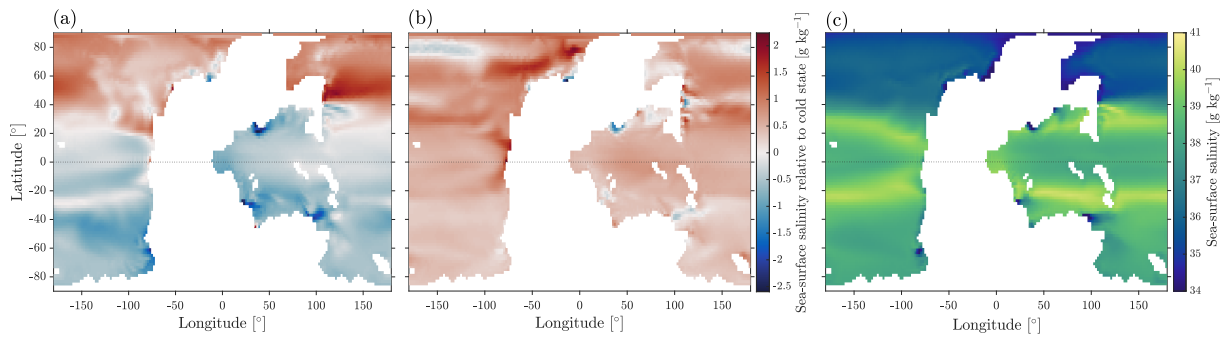Figure 2: Precipitation (up) and evaporation (bottom) for *(a, d)*: hot - cold; *(b, e)*: warm - cold; *(c, f)* cold).

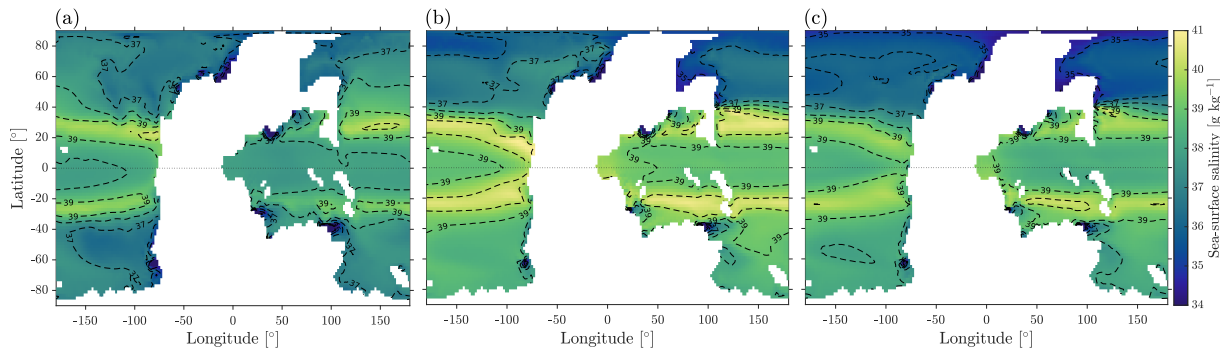Figure 3: Difference plots for the salinity field: *(a)* hot - cold; *(b)* warm - cold; *(c)* cold.

Figure 4: Salinity field for *(a)* hot; *(b)* warm; *(c)* cold states.

References

Berner, R. A. (2006). Geocarbsulf: A combined model for phanerozoic atmospheric o2 and co2. *Geochimica et Cosmochimica Acta*, *70*(23), 5653–5664. A Special Issue Dedicated to Robert A. Berner. URL https://www.sciencedirect.com/science/article/pii/S0016703706002031

Brunetti, M., Kasparian, J., & Vérard, C. (2019). Co-existing climate attractors in a coupled aquaplanet.

Climate Dynamics, *53*(9-10), 6293–6308.
URL http://link.springer.com/10.1007/s00382-019-04926-7

Brunetti, M., & Ragon, C. (2023). Attractors and bifurcation diagrams in complex climate models. *Phys. Rev. E*, *107*, 054214.
URL https://link.aps.org/doi/10.1103/PhysRevE.107.054214

Brunetti, M., & Vérard, C. (2018). How to reduce long-term drift in present-day and deep-time simulations? *Climate dynamics*, *50*(11-12), 4425–4436.

Brühwiler, T., Bucher, H., Brayard, A., & Goudemand, N. (2010). High-resolution biochronology and diversity dynamics of the early triassic ammonoid recovery: The smithian faunas of the northern indian margin. *Palaeogeography, Palaeoclimatology, Palaeoecology*, *297*(2), 491–501.
URL https://www.sciencedirect.com/science/article/pii/S0031018210005274

Campbell, I. H., Czamanske, G. K., Fedorenko, V. A., Hill, R. I., & Stepanov, V. (1992). Synchronism of the siberian traps and the permian-triassic boundary. *Science*, *258*(5089), 1760–1763.
URL https://www.science.org/doi/abs/10.1126/science.258.5089.1760

Campin, J.-M., Marshall, J., & Ferreira, D. (2008). Sea ice–ocean coupling using a rescaled vertical coordinate z*. *Ocean Modelling*, *24*(1), 1–14.
URL https://www.sciencedirect.com/science/article/pii/S1463500308000553

Foster, G., Royer, D., & Lunt, D. (2017). Future climate forcing potentially without precedent in the last 420 million years. *Nature Communications 8*, *14845*.

Galfetti, T., Bucher, H., Ovtcharova, M., Schaltegger, U., Brayard, A., Brühwiler, T., Goudemand, N., Weissert, H., Hochuli, P. A., Cordey, F., & Guodun, K. (2007). Timing of the early triassic carbon cycle perturbations inferred from new u–pb ages and ammonoid biochronozones. *Earth and Planetary Science Letters*, *258*(3), 593–604.
URL https://www.sciencedirect.com/science/article/pii/S0012821X0700252X

Goudemand, N., Romano, C., Leu, M., Bucher, H., Trotter, J. A., & Williams, I. S. (2019). Dynamic interplay between climate and marine biodiversity upheavals during the early triassic smithian -spathian biotic crisis. *Earth-Science Reviews*, *195*, 169–178.
URL https://www.sciencedirect.com/science/article/pii/S0012825218302563

Gough, D. O. (1981). Solar interior structure and luminosity variations. In V. Domingo (Ed.) *Physics of Solar Variations*, (pp. 21–34). Dordrecht: Springer Netherlands.

Harrison, S. P., & Prentice, C. I. (2003). Climate and co2 controls on global vegetation distribution at the last glacial maximum: analysis based on palaeovegetation data, biome modelling and palaeoclimate simulations. *Global Change Biology*, *9*(7), 983–1004.

Hermann, E., Hochuli, P. A., Bucher, H., Brühwiler, T., Hautmann, M., Ware, D., & Roohi, G. (2011). Terrestrial ecosystems on north gondwana following the end-permian mass extinction. *Gondwana Research*, *20*(2), 630–637.
URL https://www.sciencedirect.com/science/article/pii/S1342937X1100030X

Jackson, L. C., & Wood, R. A. (2018). Hysteresis and resilience of the amoc in an eddy-permitting gcm. *Geophysical Research Letters*, *45*(16), 8547–8556.
URL https://agupubs.onlinelibrary.wiley.com/doi/abs/10.1029/2018GL078104

Joachimski, M. M., Müller, J., Gallagher, T. M., Mathes, G., Chu, D. L., Mouraviev, F., Silantiev, V., Sun, Y. D., & Tong, J. N. (2022). Five million years of high atmospheric CO2 in the aftermath of the Permian-Triassic mass extinction. *Geology*, *50*(6), 650–654.
URL https://doi.org/10.1130/G49714.1

Kaplan, J. O. (2001). Geophysical applications of vegetation modeling. Tech. rep., Lund University.

Lauritzen, P. H., & Williamson, D. L. (2019). A total energy error analysis of dynamical cores and physics-dynamics coupling in the community atmosphere model (cam). *Journal of Advances in Modeling Earth Systems*, *11*(5), 1309–1328.
URL https://agupubs.onlinelibrary.wiley.com/doi/abs/10.1029/2018MS001549

Lembo, V., Lunkeit, F., & Lucarini, V. (2019). Thediato (v1.0) – a new diagnostic tool for water, energy and entropy budgets in climate models. *Geoscientific Model Development*, *12*(8), 3805–3834.
URL https://gmd.copernicus.org/articles/12/3805/2019/

Lenton, T. M., Daines, S. J., & Mills, B. J. (2018). Copse reloaded: An improved model of biogeochemical cycling over phanerozoic time. *Earth-Science Reviews*, *178*, 1–28.
URL https://www.sciencedirect.com/science/article/pii/S0012825217304117

Leu, M., Bucher, H., & Goudemand, N. (2019). Clade-dependent size response of conodonts to environmental changes during the late smithian extinction. *Earth-Science Reviews*, *195*, 52–67.
URL https://www.sciencedirect.com/science/article/pii/S0012825218302216

Liepert, B. G., & Previdi, M. (2012). Inter-model variability and biases of the global water cycle in cmip3 coupled climate models. *Environmental Research Letters*, *7*(1), 014006.

Lucarini, V., & Ragone, F. (2011). Energetics of climate models: Net energy balance and meridional enthalpy transport. *Reviews of Geophysics*, *49*(1), RG1001.
URL https://agupubs.onlinelibrary.wiley.com/doi/abs/10.1029/2009RG000323

MacLeod, N. (2014). The geological extinction record: History, data, biases, and testing. In *Volcanism, Impacts, and Mass Extinctions: Causes and Effects*. Geological Society of America.
URL https://doi.org/10.1130/2014.2505(01)

Malmierca-Vallet, I., Sime, L. C., & the D-O community members (2023). Dansgaard–oeschger events in climate models: review and baseline marine isotope stage 3 (mis3) protocol. *Climate of the Past*, *19*(5), 915–942.
URL https://cp.copernicus.org/articles/19/915/2023/

Mauritsen, T., Stevens, B., Roeckner, E., Crueger, T., Esch, M., Giorgetta, M., Haak, H., Jungclaus, J., Klocke, D., Matei, D., Mikolajewicz, U., Notz, D., Pincus, R., Schmidt, H., & Tomassini, L. (2012). Tuning the climate of a global model. *Journal of Advances in Modeling Earth Systems*, *4*, M00A01.

Molteni, F. (2003). Atmospheric simulations using a GCM with simplified physical parametrizations. I: model climatology and variability in multi-decadal experiments. *Climate Dynamics*, *20*(2), 175–191.
URL http://link.springer.com/10.1007/s00382-002-0268-2

Nowak, H., Vérard, C., & Kustatscher, E. (2020). Palaeophytogeographical patterns across the permian–triassic boundary. *Frontiers in Earth Science*, *8*, 613350.

Orchard, M. J. (2007). Conodont diversity and evolution through the latest permian and early triassic upheavals. *Palaeogeography, Palaeoclimatology, Palaeoecology*, *252*(1), 93–117.
URL https://www.sciencedirect.com/science/article/pii/S0031018207001113

Pascale, S., Gregory, J. M., Ambaum, M. H., & Tailleux, R. (2012). A parametric sensitivity study of entropy production and kinetic energy dissipation using the famous aogcm. *Climate dynamics*, *38*(5-6), 1211–1227.

Payne, J. L., Lehrmann, D. J., Wei, J., Orchard, M. J., Schrag, D. P., & Knoll, A. H. (2004). Large perturbations of the carbon cycle during recovery from the end-permian extinction. *Science*, *305*(5683), 506–509.
URL https://www.science.org/doi/abs/10.1126/science.1097023

Peltier, W. R., & Vettoretti, G. (2014). Dansgaard-oeschger oscillations predicted in a comprehensive model of glacial climate: A "kicked" salt oscillator in the atlantic. *Geophysical Research Letters*, *41*(20), 7306–7313.
URL https://agupubs.onlinelibrary.wiley.com/doi/abs/10.1002/2014GL061413

Ragon, C., Lembo, V., Lucarini, V., Vérard, C., Kasparian, J., & Brunetti, M. (2022). Robustness of competing climatic states. *Journal of Climate*, *35*(9), 2769 – 2784.
URL https://journals.ametsoc.org/view/journals/clim/35/9/JCLI-D-21-0148.1.xml

Raup, D. M. (1979). Size of the permo-triassic bottleneck and its evolutionary implications. *Science*, *206*(4415), 217–218.
URL https://www.science.org/doi/abs/10.1126/science.206.4415.217

Reichow, M. K., Pringle, M., Al'Mukhamedov, A., Allen, M., Andreichev, V., Buslov, M., Davies, C., Fedoseev, G., Fitton, J., Inger, S., Medvedev, A., Mitchell, C., Puchkov, V., Safonova, I., Scott, R., & Saunders, A. (2009). The timing and extent of the eruption of the siberian traps large igneous province: Implications for the end-permian environmental crisis. *Earth and Planetary Science Letters*, *277*(1), 9–20.
URL https://www.sciencedirect.com/science/article/pii/S0012821X08006389

Renne, P. R., Black, M. T., Zichao, Z., Richards, M. A., & Basu, A. R. (1995). Synchrony and causal relations between permian-triassic boundary crises and siberian flood volcanism. *Science*, *269*(5229), 1413–1416.
URL https://www.science.org/doi/abs/10.1126/science.269.5229.1413

Retallack, G. J., Sheldon, N. D., Carr, P. F., Fanning, M., Thompson, C. A., Williams, M. L., Jones, B. G., & Hutton, A. (2011). Multiple early triassic greenhouse crises impeded recovery from late permian mass extinction. *Palaeogeography, Palaeoclimatology, Palaeoecology*, *308*(1), 233–251.
URL https://www.sciencedirect.com/science/article/pii/S0031018210005924

Romano, C., Goudemand, N., Vennemann, T. W., Ware, D., Schneebeli-Hermann, E., Hochuli, P. A., Brühwiler, T., Brinkmann, W., & Bucher, H. (2013). Climatic and biotic upheavals following the end-permian mass extinction. *Nature Geoscience*, *6*(1), 57–60.

Royer, D. L., Berner, R. A., Montañez, I. P., Tabor, N. J., Beerling, D. J., et al. (2004). Co~ 2 as a primary driver of phanerozoic climate. *GSA today*, *14*(3), 4–10.

Salzmann, U., Haywood, A. M., Lunt, D. J., Valdes, P. J., & Hill, D. J. (2008). A new global biome reconstruction and data-model comparison for the middle pliocene. *Global Ecology and Biogeography*, *17*(3), 432–447.
URL https://onlinelibrary.wiley.com/doi/abs/10.1111/j.1466-8238.2008.00381.x

Schneebeli-Hermann, E. (2020). Regime shifts in an early triassic subtropical ecosystem. *Frontiers in Earth Science*, *8*.
URL https://www.frontiersin.org/articles/10.3389/feart.2020.588696

Sellwood, B. W., & Valdes, P. J. (2008). Jurassic climates. *Proceedings of the Geologists' Association*, *119*(1), 5–17.
URL https://www.sciencedirect.com/science/article/pii/S0016787859800687

Stanley, S. M. (2016). Estimates of the magnitudes of major marine mass extinctions in earth history. *Proceedings of the National Academy of Sciences*, *113*(42), E6325–E6334.
URL https://www.pnas.org/doi/abs/10.1073/pnas.1613094113

Sun, Y., Joachimski, M. M., Wignall, P. B., Yan, C., Chen, Y., Jiang, H., Wang, L., & Lai, X. (2012). Lethally hot temperatures during the early triassic greenhouse. *Science*, *338*(6105), 366–370.
URL https://www.science.org/doi/abs/10.1126/science.1224126

Trenberth, K. E. (2020). Understanding climate change through earth's energy flows. *Journal of the Royal Society of New Zealand*, *50*(2), 331–347.
URL https://doi.org/10.1080/03036758.2020.1741404

Widmann, P., Bucher, H., Leu, M., Vennemann, T., Bagherpour, B., Schneebeli-Hermann, E., Goudemand, N., & Schaltegger, U. (2020). Dynamics of the largest carbon isotope excursion during the early triassic biotic recovery. *Frontiers in Earth Science*, *8*.
URL https://www.frontiersin.org/articles/10.3389/feart.2020.00196

Ziegler, A. M. (1990). Phytogeographic patterns and continental configurations during the permian period. *Geological Society, London, Memoirs*, *12*(1), 363–379.
URL https://www.lyellcollection.org/doi/abs/10.1144/GSL.MEM.1990.012.01.35